Astron. Astrophys. 249, 574–580 (1991)

ASTRONOMY AND ASTROPHYSICS

Variability of accretion discs around compact objects

J.P. Lasota [1] **and D. Pelat** [2]

[1] UPR 176-CNRS; DARC, Observatoire de Paris, Section de Meudon, F-92195 Meudon Cedex, France
[2] URA 173; DAEC, Observatoire de Paris, Section de Meudon, F-92195 Meudon Cedex, France

Received November 7, 1990; accepted January 29, 1991

Abstract. We study the variability of inner regions of accretion discs around compact objects. This analysis is analogous to the approach of Taam & Lin (1984). Only the case in which viscous stresses are proportional to the total pressure is investigated. We find that in the (locally) thermally unstable regime inner regions of the disc always become effectively optically thin ($\tau_{\rm eff} < 1$) and that the evolution and dics structure depend critically on the treatment of the transitions between optically thick and optically thin configurations.

Key words: accretion – accretion discs – black holes – X-rays: binaries

1. Introduction

Accretion disc play a central role in many astrophysical objects and phenomena. Their presence is well established in cataclysmic variables (CVs) and low mass X-ray binaries (LMBXs) and there is rather strong evidence that they could be present in active galactic nuclei (AGNs) (for recent reviews see Meyer et al. 1989; Bertout et al. 1991). Models of accretion discs suffer mainly from the ignorance of the nature of the physical processes which are responsible for driving accretion. Normally one invokes turbulent and/or magnetic viscosities or spiral shocks (see e.g. Meyer et al. 1989) but for most practical purposes the α prescription of Shakura & Sunyaev (1973) is used. Despite their crudeness α models of geometrically thin accretion discs have been used with success in the description of some properties of CVs, LMBXs and AGNs.

In the case of high accretion rates, however, the status of the standard Shakura-Sunyaev model is less certain: the inner regions of the disc become both thermally (Pringle et al. 1973) and viscously (Lightman & Eardley 1974) unstable. Both types of instability occur when radiation provides a substantial contribution to the total pressure:

$$1-\beta = 1-\frac{P_{\rm g}}{P_{\rm g}+P_{\rm r}} > 0.6$$

(Shakura & Sunyaev 1976), where $P_{\rm r}$ is the radiation pressure and $P_{\rm g}$ is the gas pressure. This instability occurs only if the viscous stresses are proportional to the total pressure $P_{\rm T}$. The evolution of this type of disk instabilities is unclear. On the one hand it has been speculated that the temperature runaway leads to a two-temperature disc in which very hot ions provide a dominant gas pressure contribution while electrons are cooled by inverse Compton radiation (Shapiro et al. 1976). On the other hand Taam & Lin (1984, hereafter TL) suggested that nonlocal (radial) energy transport may play an important role in stabilizing the regions of the disc that are unstable according to the local criteria (see Clarke 1988 for a discussion of these problems). Abramowicz (1981) pointed out that in the case of accretion onto a black hole the transonic character of the flow at the inner edge of the disc (a general relativistic effect) may provide an efficient stabilizing mechanism. Abramowicz et al. (1988; see also Lasota 1989) constructed a family of solutions ("slim discs") which generalize the Shakura-Sunyaev solution to the case where the radial flow is transonic. Finally, preliminary results by Matsumoto et al. (1989) show that due to onset of a thermal instability in radiation pressure dominated regions a geometrically thin disc evolves into a slim disc. Calculations by Matsumoto et al. (1989) suggest that the disc could enter into a limit cycle.

In this paper we try to understand the TL results which suggest that non-local effects can stabilize an *optically thick* and *geometrically thin* accretion disc in the regime where it is locally unstable. We show that although the non-local effects invoked by TL are important for the time evolution of the disc they are *not* sufficient to suppress the instability predicted by the local analysis. The limit cycle behaviour obtained by TL results from the interpolation between the optically thick radiative cooling formula and the one used in the optically thin case. This interpolation produces an unphysical (at least in this approximation) "upper branch" of stable disc equilibria. We find therefore that there is no apparent contradiction between TL and our results on the one hand and those of Matsumoto et al. (1989) on the other since they refer to different sets of equations. One also concludes that relativistic effects are crucial for the existence of a "real" upper branch, as discussed in Abramowicz et al. (1988). In Sect. 2 we formulate the problem and Sect. 3 presents methods of its solution. Section 4 contains the results and discussion.

2. Formulation of the problem

2.1. Basic equations

We neglect the disc self-gravity and use Newtonian potential to describe the gravity pull of the central object. The evolution of surface density $\Sigma(r) = 2\varrho H$ (where ϱ is the gas density and H the

Send offprint requests to: J.P. Lasota

half-thickness of the disc) is governed by the diffusion equation (Pringle 1981):

$$\frac{\partial \Sigma}{\partial t} = \frac{3}{r}\frac{\partial}{\partial r}\left[r^{1/2}\frac{\partial}{\partial r}\left(\nu \Sigma r^{1/2}\right)\right], \tag{1}$$

where ν is the kinematic viscosity coefficient. Equation (1) is derived from mass and angular momentum conservation assuming that the disc azimuthal motion is keplerian. The kinematic viscosity coefficient is expressed by a Shakura-Sunyaev type α-law:

$$\nu = \frac{2}{3}\alpha\frac{c_s^2}{\Omega}, \tag{2}$$

where $\alpha \leqq 1$ and $c_s = \left(\frac{P_T}{\varrho}\right)^{1/2}$ is the adiabatic speed of sound.

Following TL the time dependent energy equation is:

$$C_v \varrho\left[\frac{\partial T}{\partial t} + v\frac{\partial T}{\partial r} - (\Gamma_3 - 1)\frac{T}{\Sigma}\left(\frac{\partial \Sigma}{\partial t} + v\frac{\partial \Sigma}{\partial r}\right)\right]$$

$$= Q^+ - Q^- - \frac{\partial (r F_r)}{r \partial r}, \tag{3}$$

where

$$C_v = \frac{\Re}{\mu(\gamma - 1)}\frac{12(\gamma - 1)(1-\beta) + \beta}{\beta}$$

is the specific heat per unit volume, T the central disc temperature, v the radial speed,

$$\Gamma_3 = 1 + \frac{(4 - 3\beta)(\gamma - 1)}{\beta + 12(\gamma - 1)(1-\beta)}, \quad \Omega = \left(\frac{GM}{r^3}\right)^{1/2}$$

the (keplerian) orbital speed, Q^+ and Q^- are the energy generation rate and the vertical radiative cooling respectively (both per unit volume), F_r is the radial radiative flux, γ is the ratio of specific heats (later assumed to be 5/3), $\Re$ is the gas constant and

$$\mu \approx \frac{1}{(2X + \frac{3}{4}Y + \frac{1}{2}Z)}$$

is the mean molecular weight (≈ 0.62, i.e. we take Population I abundances $X = 0.7$, $Y = 0.28$ and $Z = 0.02$). Equation (3) is a vertically averaged form of the energy equation, in particular the energy generation rate by viscous stresses has the form:

$$Q^+ = \frac{9}{4}\varrho \nu \Omega^2, \tag{4}$$

and the vertical radiative cooling is given by:

$$Q^- = \frac{2F_z}{H}, \tag{4a}$$

where F_z is the vertical component of the radiative flux. The radial velocity is given by:

$$v = -\frac{3}{\Sigma r^{1/2}}\frac{\partial}{\partial r}(\nu \Sigma r^{1/2}). \tag{5}$$

Note that advective terms are present in Eq. (3).

2.2. *Radiative cooling*

In the effectively optically thick case the vertical radiation flux from one surface of the disc is:

$$F_z = \frac{2acT^4}{3(\kappa_{ff} + \kappa_e)\Sigma}, \tag{6}$$

where $\kappa_{ff} = 6.13\ 10^{22}\varrho T^{-7/2}$ is the free-free Rosseland mean opacity coefficient, and $\kappa_e = 0.34$ the electron scattering opacity. Equation (6) is valid only in the optically thick case, i.e. when

$$\tau_{eff} = (\kappa_e \kappa_{ff})^{1/2}\frac{\Sigma}{2} \gg 1. \tag{7}$$

2.2.1. The optically thin case: the Taam & Lin approach

In the optically thin case we first follow TL in adopting the comptonized free-free formula:

$$F_z = A\,\varepsilon_{ff} H \tag{8}$$

where A is the Compton enhancement factor and ε_{ff} the free-free emission coefficient per unit volume (for detailed formulae see TL). Whenever $A\tau_{eff}^2 > 1$ we use Eq. (6) while for $A\tau_{eff}^2 < 1$ we use an interpolation between the two cases. The consequences of the interpolation are discussed in Sect. 4.

As in TL the radial flux is expressed by the formula:

$$F_r = \frac{-4acT^3}{3\kappa\varrho}\frac{\partial T}{\partial r} \tag{9}$$

in the optically thick regions and zero elsewhere. In the optically thin regions the radiation pressure can be neglected.

2.2.2. The "grey disc" approximation

In order to study the disc behaviour near $\tau_{eff} \approx 1$ in more details, we modelled its vertical structure by a grey, isothermal, scattering atmosphere in the Eddington approximation (see e.g. Rybicki & Lightman 1979). The boundary condition adapted to the disc symmetry are: $I_+ (\tau_{eff} = 0)$ and $I_+ = I_-$ at $\tau_{eff} = \tau_{max}$, where

$$I^{\pm} = J \pm \frac{1}{\sqrt{3}}\frac{\partial J}{\partial r}$$

and J is the mean intensity. The radiative flux is given by:

$$F_z = \frac{4\pi}{\sqrt{3}}J(0) = B(T)\left(1 - \frac{e^{-\tau_{max}} + e^{\tau_{max}}}{e^{\tau_{max}}E_+ + e^{-\tau_{max}}E_-}\right), \tag{10}$$

where

$$E_\pm = 1 \pm \varepsilon^{1/2},\ \varepsilon = \frac{\kappa_{ff}}{\kappa_{ff} + \kappa_e} \text{ and } \tau_{max} = \sqrt{3}(\tau_{ff}(\tau_{ff} + \tau_e))^{1/2}$$

is the optical depth of the disc at the midplane. Note that (κ_{ff} is the *Planck mean* opacity) whereas in Sect. 2.2.1 the Rosseland mean has been used (κ_{ff} (Rosseland) $\approx 0.1\,\kappa_{ff}$ (Planck)).

The radiation pressure is then:

$$P_r = \frac{4\pi}{3c}J(\tau_{max}) = B(T)\left(1 - \frac{2}{e^{\tau_{max}}E_+ + e^{-\tau_{max}}E_-}\right). \tag{11}$$

For the radiative flux we take Eq. (6) when $\tau_{max} > 1$, Eq. (10) is used when $\tau_{max} \approx 1$ and $\tau_{max} < 1$. For the radiative pressure we always use Eq. (11) whatever the value of τ_{max} since it is valid in the two limiting cases $\tau_{max} \to 0$ and $\tau_{max} \to \infty$. The validity of the second limit is due to the fact that in Eq. (11) the pressure is evaluated at τ_{max} so that in the optically thick limit one obtains the radiative pressure corresponding to the midplane temperature. For obvious reasons the limit $\tau_{max} \to \infty$ of Eq. (10) does not give the correct result for the radiative flux. In the the limit $\tau \to 0$ however one obtains the flux as given by Eq. (8).

3. Numerical methods and boundary conditions

We introduce dimensionless variables $x=(r/r_{\max})^{1/2}$ and $t^*=t\Omega_{\max}$ where $r_{\max}$ is the maximum disc radius, $\Omega_{\max}=(GM/r_{\min}^3)^{1/2}$, where $r_{\min}$ is the minimum disc radius. The surface density variable is $S=\Sigma x$. Dimensionless viscosity coefficient takes the form: $\nu^*=\frac{3}{4}\,\nu/\Omega_{\max}r_{\max}^2$. For other variables and the form of equations see Appendix.

At the outer boundary condition it is assumed that $\dot{M}=\dot{M}_{\rm out}=$ const. The inner boundary condition is formulated by $\nu\Sigma=0$, which means that the matter arriving at the inner edge of the disc is directly accreted on to the central object (viscous stresses vanish). If one puts $F_r=0$ the energy equation does not require an inner boundary condition (TL impose conditions connected with the numerical stability of their calculations; in our case such condition are not needed). The inner boundary is fixed at $r=3r_G$, where $r_G=2GM/c^2$ is the Schwarzschild radius although we work in the framework of newtonian gravity. To calculate the evolution of the unstable disc we use an explicit finite difference numerical method similar to the one described in Papaloizou et al. (1973). The disc is divided into 70 concentric zones with equal $\Delta r^{1/2}$ spacing. All grid points are contained between $r_{\min}$ and $r_{\max}$.

In all calculations we put $\alpha=1$ and $M=1\,M_\odot$. The stationary initial disc configuration is computed with an implicit method.

4. Results and discussion

4.1. The TL approach

Since we are solving equations for variables Σ and T we find it convenient to represent the solutions at given disc radius r in the Σ, T plane. Note that here the temperature T is the central (midplane) temperature and not the effective temperature which is frequently used in the diagrams representing the disc equilibria ("S-curves") and accretion disc evolution in dwarf novae.

The evolution of the disc in its third zone (at radius $2\ 10^6$ cm) is shown on Fig. 1. In this case $\dot{M}_{\rm out}=2.8\ 10^{16}\,{\rm g\,s^{-1}}$. At the beginning both Σ and T increase following the equilibrium curve because the local value of $\dot{M}<\dot{M}_{\rm out}$. At $T=1.58\ 10^7$ K and $\Sigma=1047\,{\rm g\,cm^{-2}}$ i.e. when $\beta\approx 0.4$, (point S_2) no stable equilibrium exists anymore and the system evolve at almost constant surface density and finds an (quasi-)equilibrium at $T\approx 2.1\ 10^7$ K (point S_3). After reaching this point the system oscillates along an upper equilibrium branch ($S_3\,S_4$). This is the stage when non-local effects enter into the game: in a way analogous to the one described in TL, a heat front propagates outward increasing the local accretion rate in subsequent zones. Matter entering and leaving a given zone leads to oscillations in Σ and T. On the upper branch (whose origin is discussed below) the thermal time $t_{\rm th}$ is comparable to the viscous time $t_{\rm visc}$ so that oscillations are not unexpected. These oscillations are seen in the light-curve only at high temporal resolution (see Fig. 2). We checked that the disc is always thin ($H/R\ll 1$) and that the radial flow is always subsonic. When the heat front dies out in the outer disc regions the inner regions cool down to the initial temperature and the cycle restarts. The resulting light-curve is shown on Fig. 2. It is very similar to the light-curves obtained by TL. The differences can be accounted for by the slightly different initial and boundary conditions (our disc reaches deeper in the potential well of the central object).

The real surprise comes from the presence of an apparent upper branch of stable equilibria. In the standard model of accretion discs (Shakura & Sunyaev 1973) no such branch is present (see e.g. Meyer 1986). A clue to what is happening is seen on Fig. 3, showing the disc equilibria and lines of constant (Rosseland mean) $\tau_{\rm eff}$. One notices immediately that the upper branch coincides with the $\tau_{\rm eff}=1$ line. It is important to point out that although the equilibrium curves are calculated assuming only local equilibrium the time-dependent calculations always include the advective terms. The comparison of Figs. 1 and 3, shows that advection terms are not important in the case of equilibrium states for $\tau>1$: the system follows almost exactly the equilibrium line and *finds no equilibrium* between points S_2 and S_3. In fact through all the calculated sequences the accretion disc *always becomes optically thin*, i.e. the optical depth Eq. (7) always becomes smaller than unity. This is not in contradiction with the results of TL (Taam, private communication). According to the TL prescription one interpolates between formulae (6) and (8). The implications of such a procedure can be seen in Fig. 4. This figure represents the difference between the volume heating (Q^+) and cooling (Q^-) as a function of temperature for a fixed surface density. This represents a constant-Σ cut through the middle of the equilibrium curve in Fig. 1 (the straight line through points ABC). The full line represents Q^+-Q^- as given by Eqs. (4) and (6) (the

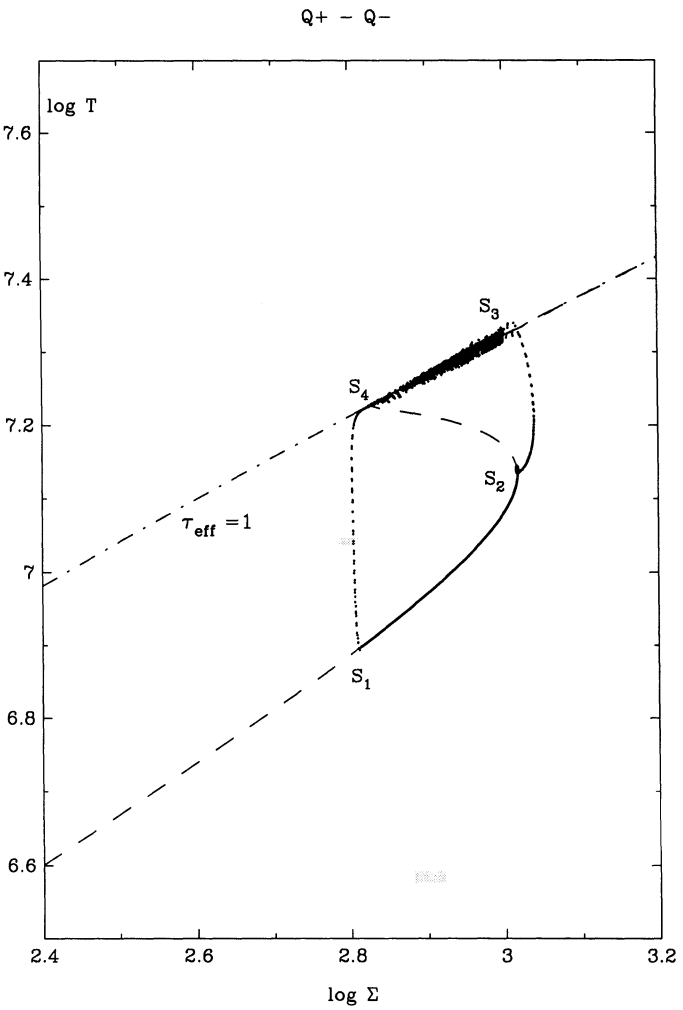

Fig. 1. The limit cycle describing the evolution of the inner zone of an accretion disc which is locally thermally unstable. Steady equilibria are represented by the dashed line, dots represent momentaneous states of disc. The system moves along the curve $S_1S_2S_3S_4S_1$

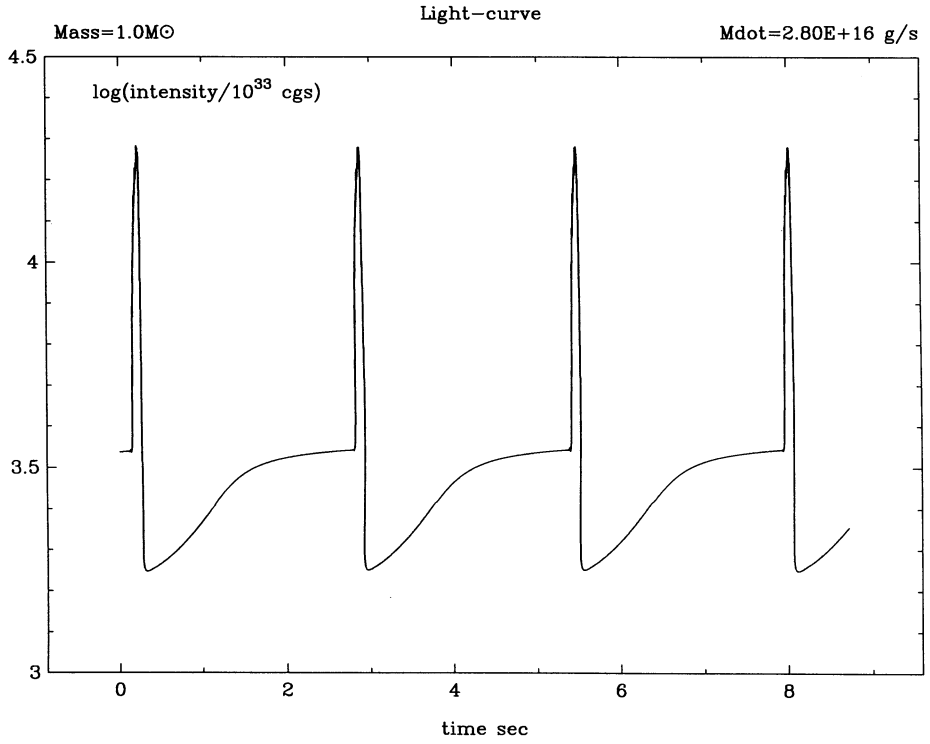

Fig. 2. Luminosity as a function of time for $\dot{M} = 2.8\ 10^{16}\,\mathrm{g\,s^{-1}}$, in the TL model

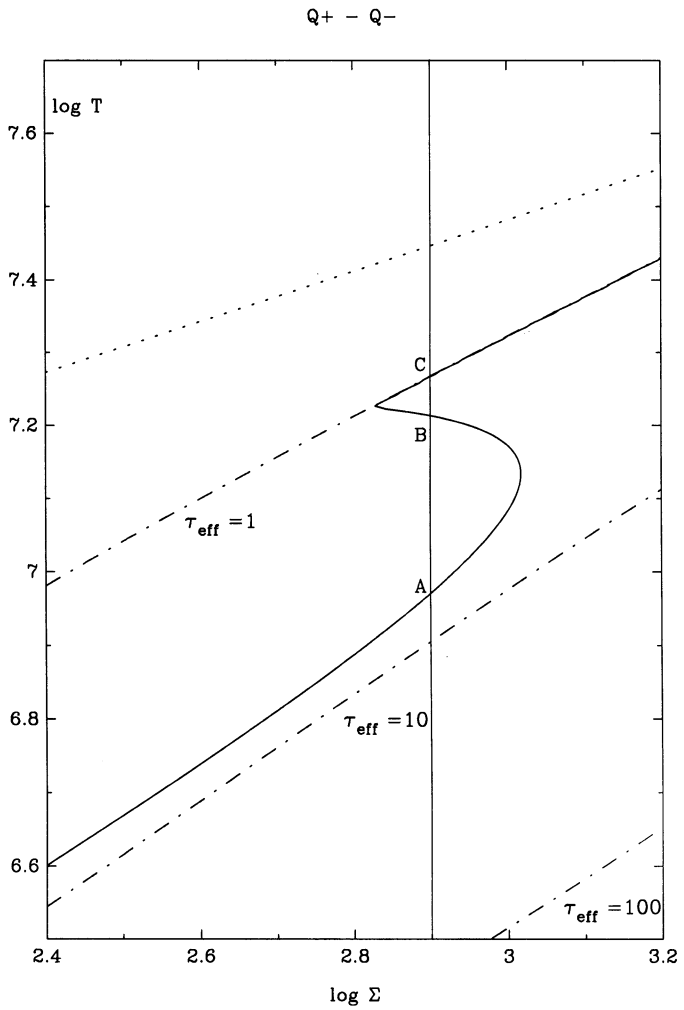

optically thick case). This line crosses zero twice at A and B, the lower root (point A) representing the stable solution. The dotted line represents the optically thin case as given by Eqs. (4) and (8) (here we keep $P_{\mathrm{rad}} \neq 0$ in the optically thin case in order to maintain a reasonable scale of the figure – this has no influence on our conclusions). The full line stops at $\tau_{\mathrm{eff}} = 1$ and the dashed-dotted line is the result of the interpolation $\tau_{\mathrm{eff}} \approx 1$. The dashed-dotted line has to cross the $Q^+ - Q^-$ line (point C) and thus creates a stable solution around optical depth $\tau_{\mathrm{eff}} = 1$. The upper branch is the result of this interpolation. This sequence of disc equilibria is clearly unphysical. The limit cycle is not due to the global effect and advection but to an artificial sequence of stable solution. Note however that this conclusion is valid only in the case of the thin disc approximation. In the framework of the slim disc models in which matter flows through a sonic point advection could stabilize the thermal runaway (Abramowicz et al. 1987, 1988; Matsumoto et al. 1989).

4.2. The grey disc approximation

An insight into the essential role played by an upper stable branch of disc equilibria may be obtained by changing the prescription for the treatment of the optically thick-optically thin transition. An exact treatment of this problem would require a fundamental modification of the approach since it would imply solving the vertical disc structure with all additional difficulties related to the viscous energy dissipation distribution in vertical direction (see

Fig. 3. Equilibrium configuration in the Σ, T (*central*) temperature plane, for the $r = 2\ 10^6$ cm zone. The upper branch is at τ_{eff} (*Rosseland*) $= 1$. The dotted line on the top represents an unphysical optically thin solution. Points A, B and C correspond the the $\Sigma =$ const cut of Fig. 4

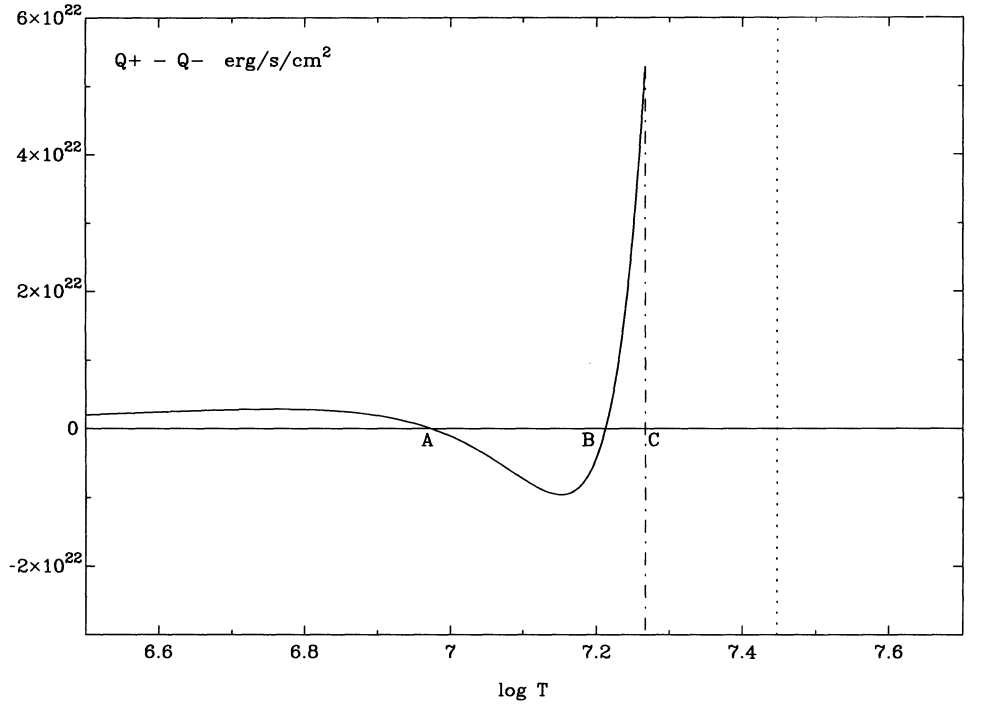

Fig. 4. Heating minus cooling curves for $\Sigma = 790\,\mathrm{g\,cm^{-2}}$ showing the possible consequences of interpolating between Eqs. (6) and (8). The continuous line represents $Q^+ - Q^-$ for $\tau > 1$. At $\tau_{\mathrm{eff}} = 1$ it joins the dashed-dotted line corresponding to an interpolation with the optically thin case (dotted line). The dashed-dotted line meets the dotted line at very low values of $Q^+ - Q^-$. Points *A*, *B*, *C* correspond to disc equilibria compare with Fig. 3

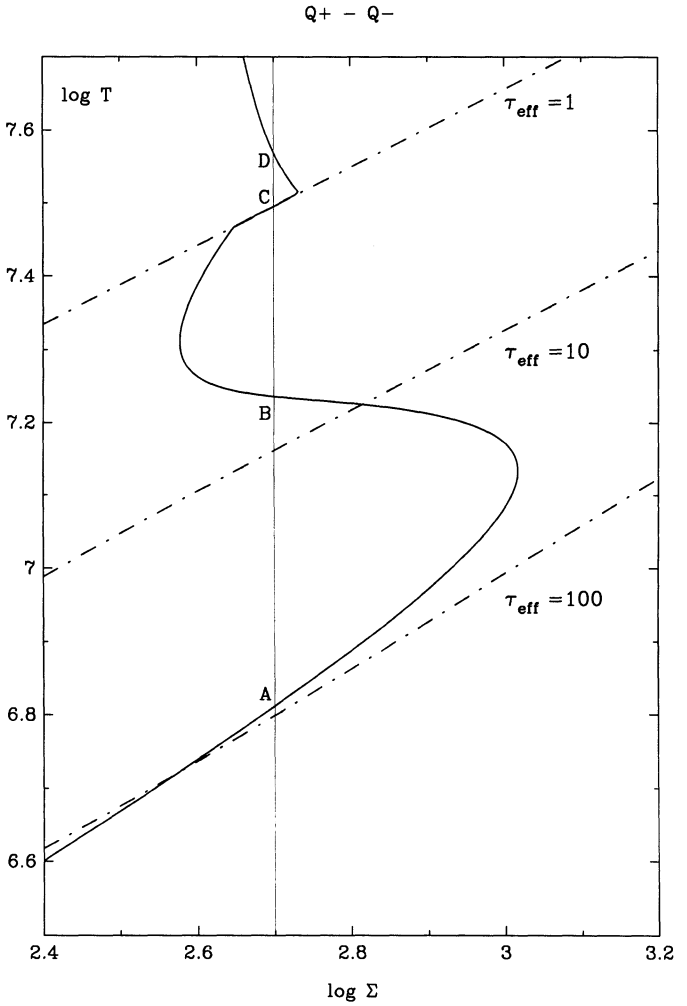

e.g. Hubeny 1989; Shaviv & Wehrse 1989). To study the disc behaviour during a thermal runaway we use the isothermal grey disc approximation described in Sect. 2.2.2. This approach has the advantage of making the equations to depend on the effective optical depth τ_{eff} contrary to the case discussed above in which τ_{eff} does not appear explicitely. Let us recall that in the grey approximation we use Eq. (11) for radiation pressure also in the optically thick case. The resulting equilibrium curve in the Σ, T plane is shown on Fig. 5. One can see that a small segment (starting at *C*) of stable upper branch is present at $\tau_{\mathrm{eff}} = 1$ (remember that here the optical depth is calculated with the Planck mean opacity). It is interesting to note that the equilibrium curve changes slope (from negative to positive) at $\log T \approx 7.3$. This is due to the use of Eq. (11) for P_{r} which takes into account optical depth effects in the calculation of the radiative pressure. However, since the flux is calculated assuming the diffusion approximation this part of the curve does not represent a self-consistent solution. On Fig. 6, we show a $Q^+ - Q^-$ cut analogous to the one from Fig. 4.

The short upper branch acts as a kind of attractor as it can be seen on Fig. 7. The parameters are the same as in Fig. 1. In the present case the system after reaching the thermally unstable state evolves towards the upper branch in a series of oscillations of decaying amplitude. These oscillations are due to non-local processes. As before, the characteristic viscous time is comparable to the thermal time: this allows rapid changes both in temperature and in surface density. The resulting light-curve is shown on Fig. 8.

Fig. 5. Equilibrium configurations (continuous line) in the Σ, T plane, for the $r = 2\ 10^6$ cm zone, with Eqs. (6), (10), and (11) used. Values of τ_{eff} (Planck) = 1, 10, and 100 are plotted (dashed-dotted lines)

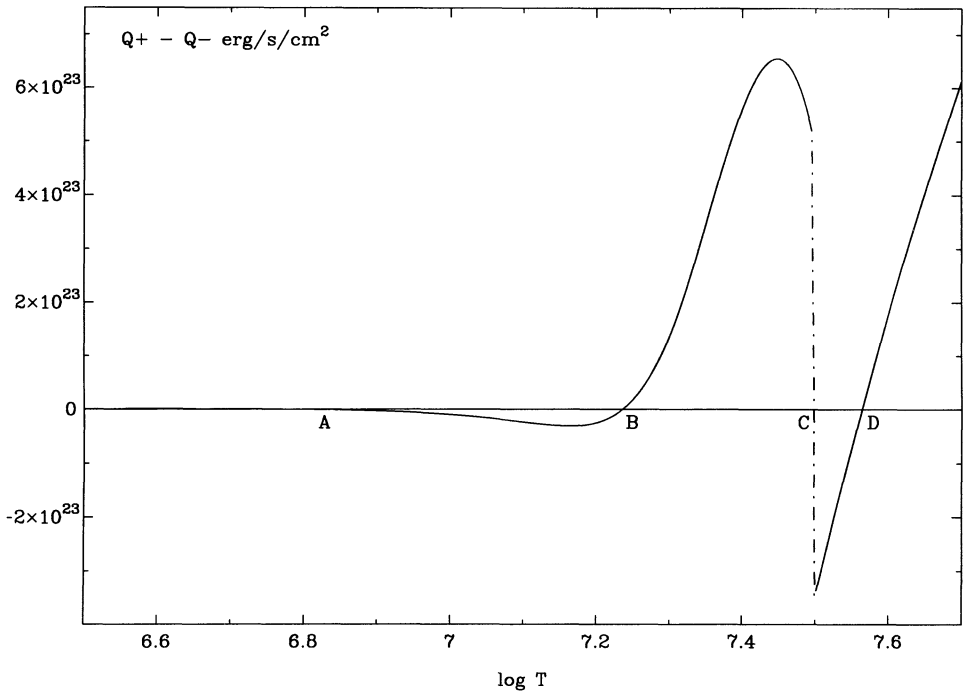

Fig. 6. Like Fig. 2 but for $\Sigma = 501\,\mathrm{g\,cm^{-2}}$ and P_r from Eq. (11). As before dashed-dotted line represents the result of interpolation. Point D corresponds to an (unstable) equilibrium state of a grey disc

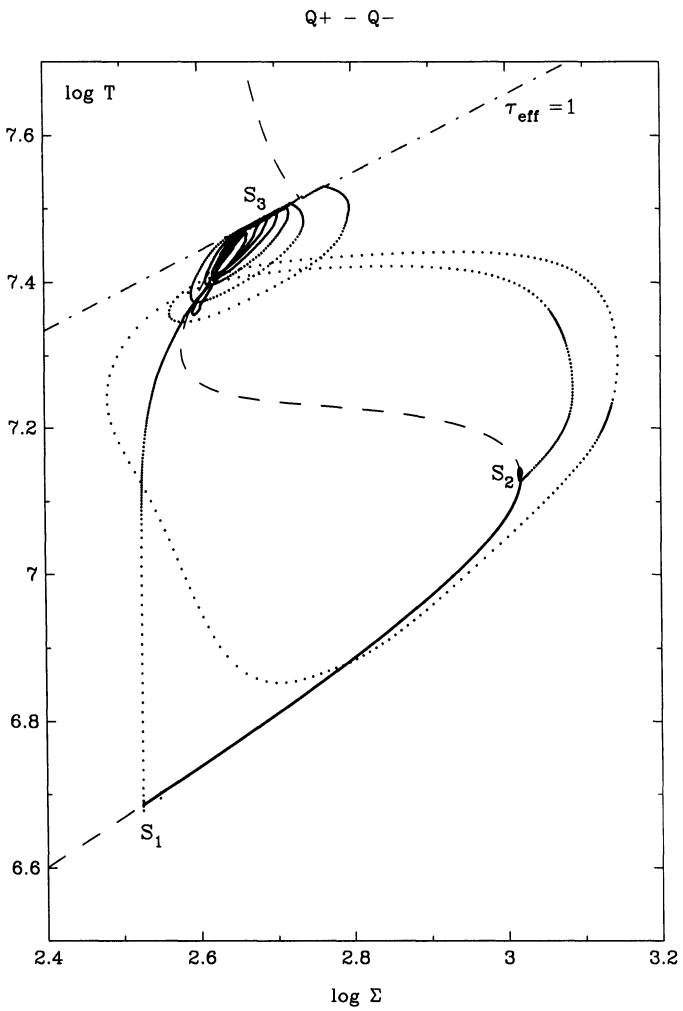

Fig. 7. The limit cycle corresponding to Fig. 6. The system moves along the dotted curve

5. Conclusions

Suppression of the upper branch leads to the disc destruction. One may conclude therefore that a thermal instability in the inner regions of an accretion disc results in a limit-cycle behaviour only if there exist high temperature stable equilibria. This is analogous to the case of dwarf novae outbursts. It is doubtful that such equilibria exist in the framework of the "standard model" of accretion discs. In some particular cases inverse Compton process could, in principle, provide the required cooling. In general the locally thermally unstable accretion discs should be described in a framework that would take into account pressure gradients etc. connected with the breaking of the thin-disc approximation.

Acknowledgements. We thank Marek Abramowicz, John Cannizzo and Mario Livio for their helpful comments and suggestions. We are also grateful to Doug Lin, Friedrich Meyer and Ron Taam for interesting discussions. JPL would like to thank the Max-Planck-Institut für Astrophysik in Garching for hospitality in October 1990 when this work was finished.

Appendix

In this appendix we present equations in normalized variables. The diffusion equation (Eq. 1) takes the form:

$$\frac{\partial S}{\partial t^*} = \frac{1}{x^2}\frac{\partial^2}{\partial x^2} v^* S. \tag{A1}$$

Equation (5) becomes:

$$v^* = -\frac{1}{S x^2}\frac{\partial}{\partial x} v^* S. \tag{A2}$$

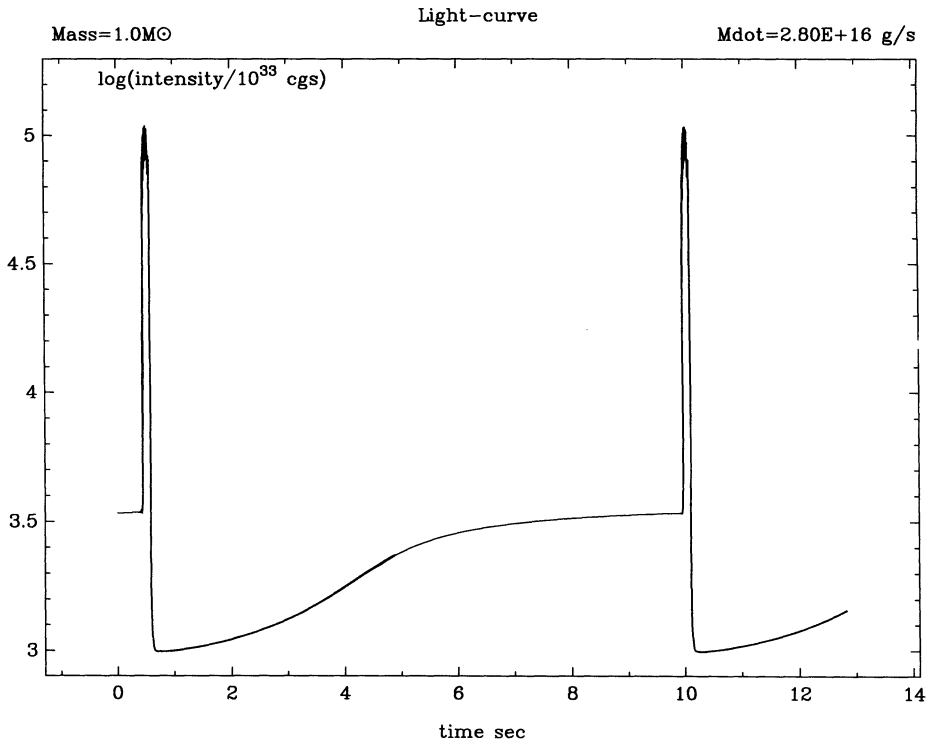

Fig. 8. Luminosity as a function of time for $\dot{M} = 2.8\ 10^{16}\,\mathrm{g\,s^{-1}}$, in the "grey-disc" model

The temperature is normalized according to the formula:

$$T^* = \frac{T}{T_0}\, x^{2/3}, \tag{A3}$$

where

$$T_0^4 = \frac{9}{4}\,\frac{1}{\kappa_e\, a\, c}\,\Omega_{\max}^3\, r_{\max}^2 \tag{A4}$$

with $a = 7.564\ 10^{-15}\,\mathrm{erg\,cm^{-3}\,K^{-4}}$ and c is the speed of light.

With $H^* = H/r_{\max}$ and $\Omega^* = \Omega/\Omega_{\max}$ the energy equation [Eq. (3)] takes the form:

$$\frac{\partial T^*}{\partial t} + v^*\,\frac{\partial T^*}{\partial x} + (\Gamma_3 - \tfrac{5}{3})\, v^*\,\frac{T^*}{x} - (\Gamma_3 - 1)\,\frac{T^*}{S}\left(\frac{\partial S}{\partial t^*} + v^*\,\frac{\partial S}{\partial x}\right)$$
$$= \frac{1}{T_0\,\Omega_{\max}\, x^{-2/3}}\,\frac{1}{C_v}\,[3\Omega_{\max}^3\, r_{\max}^2\, v^*\Omega^{*2} - 2x\,S^{-1}\,F_z], \tag{A5}$$

where in the optically thick case:

$$F_z = \frac{2\,a\,c\,T_0^4}{3\,(\kappa_e + \kappa_{ff})\,x^{5/3}}\,\frac{T^{*4}}{S}. \tag{A6}$$

References

Abramowicz M.A., 1981, Nat 294, 235

Abramowicz M.A., Czerny B., Lasota J.P., Szuszkiewicz E., 1988, ApJ 332, 646

Abramowicz M.A., Lasota J.P., Xu C., 1986, in: Variability and Instabilities of Accretion Discs, eds. G. Swarup, V.K. Kapahi, IAU Symp. No. 119, Kluwer, Dordrecht, p. 371

Bertout C., Collin-Souffrin S., Lasota J.P., Trân Thanh Vân J. (eds., 1991, Structure and Emission Properties of Accretion Disks, Proceedings of the 6 IAP/IAU Coll. No. 129, Editions Frontiéres, Paris (in press)

Clarke C.J., 1988, ApJ 235, 881

Hubeny I., 1989, in: Theory of Accretion Discs, eds. F. Meyer, W.J. Duschl, J. Frank, E. Meyer-Hofmeister, Kluwer, Dordrecht, p. 445

Lasota J.P., 1989, in: Accretion Discs and Magnetic Fields in Astrophysics, ed. G. Belvedere, Kluwer, London, p. 273

Lightman A.P., Eardley D.M., 1974, ApJ 187, L1

Matsumoto R., Kato R., Honna F., 1989, in: Theory of Accretion Disks, eds. F. Meyer, W.J. Duschl, J. Frank, E. Meyer-Hofmeister, Kluwer, Dordrecht, p. 167

Meyer F., Duschl, W.J., Frank J., Meyer-Hofmeister E., 1989, Theory of Accretion Disks, Kluwer, Dordrecht

Meyer F., 1986, in: Radiation Hydrodynamics in Stars and Compact Objects, eds. D. Mihalas, K.H.A. Winkler, Springer, Berlin Heidelberg New York, p. 249

Papaloizuo J.C.B., Faulkner J., Lin D.N.C., 1973, MNRAS 205, 487

Pringle J.E., Rees M.J., Pacholczyk A.G., 1973, A&A 29, 179

Pringle J.E., 1981, ARA&A 19, 137

Rybicki G.B., Lightman A.P., 1979, Radiative Processes in Astrophysics, Wiley, New York

Shakura N.I., Sunyaev R.A., 1973, A&A 24, 337

Shakura N.I., Sunyaev R.A., 1976, MNRAS 175, 613

Shapiro S.L., Lightman A.P., Eardley D.M., 1976, ApJ 204, 187

Shaviv G., Wehrse R., 1989, in: Theory of Accretion Disks, eds. F. Meyer, W.J. Duschl, J. Frank, E. Meyer-Hofmeister, Kluwer, Dordrecht, p. 419

Taam R.E., Lin D.N.C., 1984, ApJ 287, 761